

General Resetting Theory for Group Avoidance

Juhee Lee,¹ Seong-Gyu Yang,¹ Hye Jin Park,^{2,*} and Ludvig Lizana^{1,†}

¹*Integrated Science Lab, Department of Physics, Umeå University, Umeå, Sweden*

²*Department of Physics, Inha University, Incheon 22212, Republic of Korea*

(Dated: December 4, 2024)

We present a general theoretical framework for group resetting dynamics in multi-agent systems in a drift potential. This setup contrasts with a typical resetting problem that involves a single searcher looking for a target, with resetting traditionally studied to optimize the search time to a target. More recently, resetting has also been used as a regulatory mechanism to avoid adverse outcomes, such as preventing critically high water levels in dams or deleveraging financial portfolios. Here, we extend current resetting theories to group dynamics, with applications ranging from bacterial evolution under antibiotic pressure to multiple-searcher optimization algorithms. Our framework incorporates extreme value statistics and renewal theory, from which we derive a master equation for the center of mass distribution of a group of searchers. This master equation allows us to calculate essential observables analytically. For example, how the group’s average position depends on group size, resetting rates, drift potential strength, and diffusion constants. This theoretical approach offers a new perspective on optimizing group search and regulatory mechanisms through resetting.

In stochastic search with resetting, the traditional question is finding the optimal resetting rate that minimizes the search time to a designated target [1–5]. More recently, researchers applied resetting theory to explore the inverse problem: avoidance [6, 7]. This refers to a regulatory protocol to prevent a stochastic trajectory from reaching a specific threshold. For instance, ensuring fluctuating water levels in dams do not exceed a critical height. Another example is in finance, where resetting mechanisms could help to limit excessive leverage and rebalance portfolios.

Beyond those examples, resetting theory as a regulatory mechanism has broader applicability, particularly in scenarios involving collective behavior. One example is bacterial evolution and antibiotic resistance. When exposed to an antibiotic attack, the bacterial population drifts toward drug-resistant super-bacteria [8–11]. They achieve this by evolving their metabolisms, where the most resistant bacteria will outgrow the others and take over the population. This represents an example of group search in biological-trait space, which could be slowed down by constantly resetting the population to the least fit bacteria under antibiotics, for instance, in an artificial selection protocol [12–14]. However, finding the relevant parameters in such a scheme, such as the best resetting rate, represents a considerable challenge.

Another application of group search is in optimization [15–17]. Consider an optimization algorithm where multiple random walkers are deployed to explore a mathematical landscape in search of optima. While searching, all walkers exchange their “fitness” representing the value of the function they are optimizing. At a certain rate, the walkers reset their positions to that of the fittest one and resume the search from there. While it is intuitive that more walkers lead to shorter search times, it is difficult to estimate the optimal number of searchers and the resetting rate.

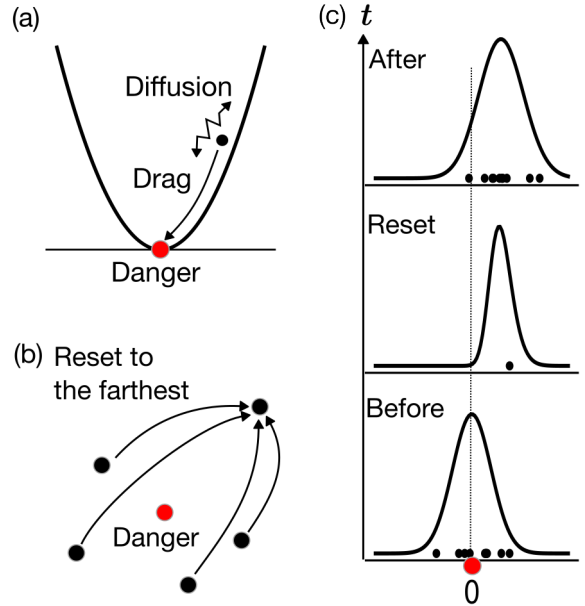


FIG. 1. Schematic figure of group resetting. (a) Each particle diffuses under a drift potential that drags them toward the danger at the minimum point. (b) When the group resets, all the particles relocate to the position of the farthest particle from the danger. (c) The position distributions before and after the group resetting event.

In this letter, we present a general theoretical framework to address group resetting in a drift potential. Specifically, we formulate a theory that incorporates both extreme value statistics and renewal theory to analyze the group resetting dynamics. From this framework, we derive a master equation governing the distribution of the group’s center of mass (ζ). Our approach provides an analytical prediction on how key parameters affect the average CM ($\langle \zeta \rangle$), such as resetting rate, group size, diffusion constant, and the strength of the drift potential.

As an example of the group resetting problem with drift, we consider n independent Brownian particles with coordinates x_i ($i = 1, \dots, n$) in a 1-dimensional harmonic potential. Each particle starts from $x_i = 0$ and diffuses with diffusion constant D in the harmonic potential $V(x) = kx^2/2$ [Fig. 1(a)]. With resetting rate r , all particles simultaneously relocate to the position $X(t)$, which corresponds to the farthest particle position from the origin at time t [Fig. 1(b)]. That is,

$$X(t) = \max(x_1(t), x_2(t), \dots, x_n(t)). \quad (1)$$

Between resetting events, the particles move according to the stochastic differential equation $dx_i = -kx_i dt + \sqrt{2D}dW_i(t)$, where the first term represents drift and $W_i(t)$ is the Wiener process.

In this setting, we develop a theory for the n -particle group resetting problem. One approach is to track the CM of the particles, defined as $x_{CM}(t) = \sum_i^n x_i(t)/n$. However, a more practical approach is to construct an effective single-particle theory that represents the CM motion using a single variable $\zeta(t)$. Below, we derive a master equation for the probability distribution $P(\zeta, t) \equiv P(\zeta, t | \zeta_0, t_0)$, where ζ_0 and t_0 are initial conditions.

The general form of the master equation for $P(\zeta, t)$ is

$$\frac{\partial}{\partial t} P(\zeta, t) = \frac{\partial}{\partial \zeta} [k\zeta P(\zeta, t)] + \frac{\partial^2}{\partial \zeta^2} \left[\frac{D}{n} P(\zeta, t) \right] - rP(\zeta, t) + rP_r(\zeta, t), \quad (2)$$

where the first two terms represent drift and diffusion in an Ornstein-Uhlenbeck process (OUP) [18, 19], with D/n being the CM diffusion constant. The last two terms describe the resetting dynamics, where the first represents the removal of the particle from ζ and the second one re-introduces it with the same rate but at a different position specified by the distribution $P_r(\zeta, t)$.

In the group resetting dynamics, the challenge lies in determining $P_r(\zeta, t)$. At the time of a reset t , all particles relocate to the resetting position $X(t)$, which results in $x_{CM}(t) = X(t)$. Since the dynamics of the effective particle $\zeta(t)$ mirrors that of the CM, $P_r(\zeta, t)$ is derived from the conditional probability density function (PDF) $K_n(X|X'; \tau)$, which describes the resetting probability to X starting from X' after time τ for a system of n particles. In the following, we first obtain $K_n(X|X'; \tau)$ by using extreme value statistics and then write $P_r(\zeta, t)$ in terms of $K_n(\zeta|\zeta'; \tau)$ replacing X into ζ .

Let us consider two sequential resets at times t' and t ($t' < t$), separated by the time interval $\tau = t - t'$. To obtain $K_n(X|X'; \tau)$ we start from the cumulative distribution $Q_n(X|X'; \tau) = \text{Prob}(X(t) \geq x_1(t), \dots, x_n(t) | X'(t'))$. Since the particles diffuse independently, $Q_n(X|X'; \tau) = [\text{Prob}(-\infty < x_i(t) \leq X(t) | X'(t'))]^n$. Using the single-particle propagator $G(y, t | X', t') = G(y | X'; \tau)$ of OUP, which describes the

probability of finding a particle at y at time t without resetting, we express $\text{Prob}(-\infty < x_i < X | X') = \int_{-\infty}^X dy G(y | X'; \tau)$. Differentiating Q_n with respect to X , we obtain

$$K_n(X|X'; \tau) = nG(X|X'; \tau) \left[\int_{-\infty}^X dy G(y|X'; \tau) \right]^{n-1}. \quad (3)$$

In the large n limit, $K_n(X|X'; \tau)$ converges to the PDF of Gumbel distribution [20–22], given by $\text{Gumbel}(y; \mu, \beta) = \frac{1}{\beta} \exp\{-(y-\mu)/\beta + \exp[-(y-\mu)/\beta]\}$, where μ and β represent the location and scale parameters, respectively. These parameters are determined by the mean \bar{y} and variance σ^2 of the OUP over the time interval τ , known to be $\bar{y}(X', \tau) = X' e^{-k\tau}$ and $\sigma^2(X', \tau) = \frac{D}{k} [1 - \exp(-2k\tau)]$ [18, 19]. Utilizing \bar{y} and σ^2 , the location and scale parameters of the Gumbel distribution become $\mu(X', \tau) = \bar{y}(X', \tau) + \sigma(X', \tau)b_n$ and $\beta(X', \tau) = \sigma(X', \tau)a_n$, where the coefficients b_n and a_n are determined by the inverse cumulative distribution $C^{-1}(\cdot)$ of a unit Gaussian distribution. This gives $b_n = C^{-1}(1-1/n)$ and $a_n = 1/b_n$. Taking all of the above into account, we find $K_n(X|X'; \tau) \sim \text{Gumbel}(X; \mu(X', \tau), \beta(X', \tau))$ in large n limit. Lastly, interpreting ζ as X , as $x_{CM} = X$ at the moment of the reset, we write $K_n(\zeta|\zeta'; \tau)$.

Next, we use renewal theory [23] to derive $P_r(\zeta, t)$ considering the last resetting event to ζ at t , starting from $\zeta_0 = 0$ at $t_0 = 0$. The resetting event at time t could be the first during the dynamics or the last among multiple events. Taking into account the waiting-time distribution of resetting $\phi(\tau)$ which satisfies $r = [\int_0^\infty \tau \phi(\tau) d\tau]^{-1}$, the first scenario occurs with probability $\Psi(t) = 1 - \int_0^t \phi(\tau) d\tau$. In this case, the resetting position is determined by $K_n(\zeta|\zeta' = 0; t)$. On the other hand, if the resetting at t is not the first event, the previous resetting happened to ζ' at $t - \tau$, and thus the resetting position ζ at t is determined by $K_n(\zeta|\zeta'; t)P_r(\zeta', t - \tau)$. This scenario happens with probability $\int_0^t d\tau \phi(\tau)$. Combining these contributions gives

$$P_r(\zeta, t) = \Psi(t)K_n(\zeta|0; t) + \int_0^t d\tau \phi(\tau) \int_{-\infty}^\infty d\zeta' K_n(\zeta|\zeta'; \tau)P_r(\zeta', t - \tau), \quad (4)$$

where $P_r(\zeta, 0) = \delta(\zeta)$. Substituting this result into Eq. (2) completes the master equation for $P(\zeta, t)$.

To corroborate our theoretical prediction of $P(\zeta, t)$, we generate stochastic trajectories of ζ . The resetting time interval τ is sampled from $\phi(\tau)$ and ζ evolves for τ according to $d\zeta = -k\zeta dt + \sqrt{\frac{2D}{n}} dW_\zeta(t)$. We numerically integrate $d\zeta$ using the Euler-Maruyama method [19, 24]. When resetting occurs after time interval τ , we draw a resetting position from $K_n(\zeta|\zeta'; \tau)$ approximated by the Gumbel distribution.

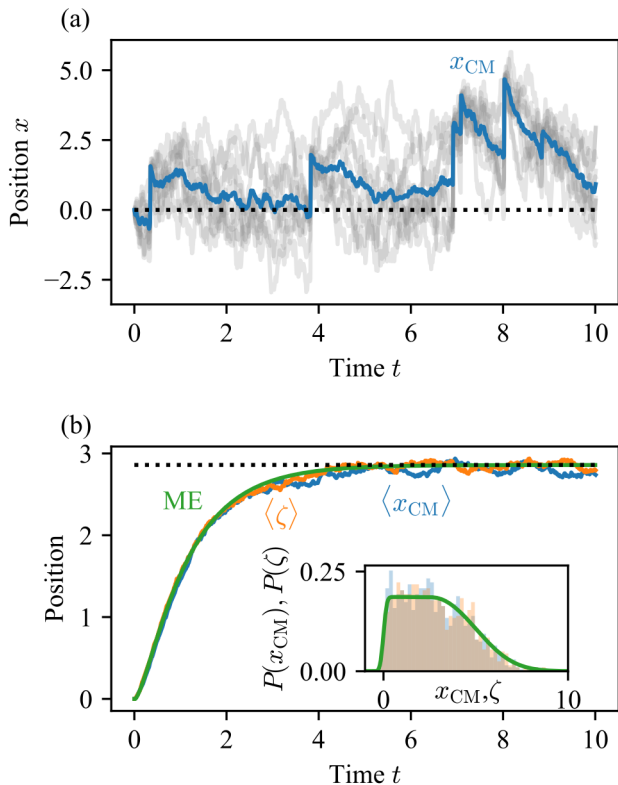


FIG. 2. Particle trajectories and average positions. (a) Simulated particle trajectories with group resetting (grey) and their center of mass (CM, blue). The sudden jumps correspond to resetting events where all the particles relocate to the farthest point from the origin. Parameters: $n = 10$, $D = 2$, $k = 1$, $r = 1$. (b) The average position over time for $n = 100$ particles. The blue line represents the average of 1000 CM trajectories, and the orange line shows stochastic simulation results of the effective single-particle. The green line corresponds to the first moment of $P(\zeta)$, which satisfies Eq. (2). The black dotted line shows $\langle \zeta \rangle_s$ [Eq.(8)]. (inset) Steady-state particle distributions. Histograms show data collected at $t = 10$ (the final time point in the simulation). The green line shows the theoretical prediction $P(\zeta)$ calculated from integrating Eq. (2) numerically.

Above, we derived the effective single-particle master equation in Eq. (2). Here, we compare it against numerical simulations. Figure 2(a) shows the position trajectories of $n = 10$ particles (grey) undergoing diffusion and group resetting ($r = 1$) to the most extreme one. When the resetting occurs, we see sudden jumps where all individual particles jump into the farthest particles' position. The figure also includes the CM (blue). In Fig. 2(b), we show the average 10^3 trajectories $\langle x_{CM}(t) \rangle$ (blue) and $\langle \zeta(t) \rangle$ of the effective particle (orange), obtained from stochastic simulations. We note that the average trajectories flatten out for a long time and become stationary.

In Fig. 2(b), we also plot the first moment $\langle \zeta(t) \rangle$ of $P(\zeta, t)$ (green, ME) alongside the simulations (blue and

orange). We calculate $\langle \zeta \rangle$ analytically from $\langle \zeta(t) \rangle = \int d\zeta \zeta P(\zeta, t)$ using Eqs. (2) and (4). This gives

$$\frac{d}{dt} \langle \zeta(t) \rangle = -(k+r) \langle \zeta(t) \rangle + r \langle \zeta_r(t) \rangle, \quad (5)$$

where $\langle \zeta_r(t) \rangle = \int_{-\infty}^{\infty} \zeta P_r(\zeta, t) d\zeta$, following

$$\begin{aligned} \langle \zeta_r(t) \rangle &= (b_n + \gamma a_n) \sqrt{\frac{D}{k}} \Psi(t) \sqrt{1 - e^{-2kt}} \\ &+ \int_0^t d\tau \phi(\tau) e^{-k\tau} \langle \zeta_r(t - \tau) \rangle \\ &+ (b_n + \gamma a_n) \sqrt{\frac{D}{k}} \int_0^t d\tau \phi(\tau) \sqrt{1 - e^{-2k\tau}}. \end{aligned} \quad (6)$$

We note excellent agreement between these expressions and our simulations.

In addition to $\langle \zeta(t) \rangle$, Fig. 2(b) shows the PDFs of x_{CM} and ζ in the long-time limit (inset). In this regime, where $P(\zeta, t \rightarrow \infty) = P_s(\zeta)$, we compute the stationary solution of Eq. (2) numerically (green). We see that $P_s(\zeta)$ aligns well with the simulations (histograms).

In the stationary limit, we also calculate $\langle \zeta \rangle_s$. To this end we found $\lim_{t \rightarrow \infty} \langle \zeta_r(t) \rangle = \langle \zeta_r \rangle_s$ from Eq. (6)

$$\langle \zeta_r \rangle_s = (b_n + \gamma a_n) \sqrt{\frac{D}{k}} \frac{r}{2k} B\left(\frac{1}{2}, \frac{r}{2k}\right). \quad (7)$$

and inserted this result into Eq. (5). This yields

$$\langle \zeta \rangle_s = (b_n + \gamma a_n) \sqrt{\frac{D}{k}} \frac{r^2}{2k(k+r)} B\left(\frac{1}{2}, \frac{r}{2k}\right), \quad (8)$$

where $B(\cdot, \cdot)$ denotes the beta function $B(u, v) = \Gamma(u)\Gamma(v)/\Gamma(u+v)$; $\Gamma(\cdot)$ is the gamma function. We plot this expression in Fig. 2(b) as the black dotted line.

The analytical expression in Eq. (8) allows us to study how the stationary position $\langle \zeta \rangle_s$ depends on key parameters. First, we investigate the impact of the group size n . The group size n is essential for the group resetting, as the theory relies on its extreme value statistics. When $n = 1$, the group search is identical to the diffusion of a single particle, resulting in $\langle \zeta \rangle_s = 0$. If there is only one particle in the system, it has nowhere to jump since there are no interactions with other particles. As n grows, however, we expect that groups with larger sizes have a higher chance to reach further distances and have growing $\langle \zeta \rangle_s$. This agrees with Fig. 3(a) showing how $\langle \zeta \rangle_s$ depends on n . We find that it has an asymptotic logarithmic increase, which can be derived by expanding Eq. (8) for large n , using $b_n \propto \sqrt{\ln n}$ [20–22].

The resetting rate r has a stronger effect on $\langle \zeta \rangle_s$ than the group size n . Without resetting ($r = 0$), we have $\langle \zeta \rangle_s = 0$, because the effective particle simply follows the OUP. With resetting, however, the situation changes. That is because the effective particle restarts its dynamics from the farthest position it could have reached, given

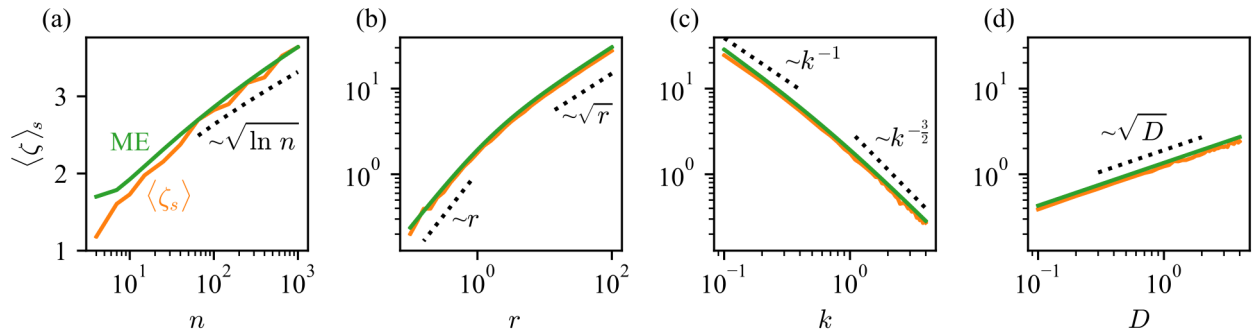


FIG. 3. The stationary mean position $\langle \zeta(t \rightarrow \infty) \rangle = \langle \zeta \rangle_s$ as a function of various parameters: (a) group size n ($D = 2$, $k = 1$, $r = 1$), (b) resetting rate r ($D = 2$, $k = 1$, $n = 10$), (c) potential strength k ($D = 2$, $n = 10$, $r = 1$), and (d) the diffusion constant D ($k = 1$, $n = 10$, $r = 1$). The orange lines represent numerical simulations, and the green lines are theoretical results obtained from Eq. (8). Dashed lines indicate scaling behaviors.

the previous resetting position. We plot the theoretical prediction (green) for different r and stochastic simulations (orange) in Fig. 3(b). It shows that $\langle \zeta \rangle_s$ increases with r but according to two different scaling behaviors.

These can be understood by the asymptotic behaviors of $\langle \zeta \rangle_s$. By expanding Eq. (8) for small $r (\ll k)$, using $B(1/2, r/2k) \approx 2k/r - 2r/k$, we find the linear expression

$$\langle \zeta \rangle_s \approx (b_n + \gamma a_n) \frac{r}{k} \sqrt{\frac{D}{k}}. \quad (9)$$

In the opposite case ($r \gg k$), we note that $\langle \zeta \rangle_s \propto \sqrt{r}$. By expanding Eq. (8) and using $B(1/2, r/2k) \sim \sqrt{2\pi k/r}$, we find

$$\langle \zeta \rangle_s \approx \frac{b_n + \gamma a_n}{k} \sqrt{\frac{\pi D r}{2}}. \quad (10)$$

This limit makes intuitive sense. During a short time interval between two resets in steady state, $\tau \approx 1/r \ll 1$, the particle drifts toward the origin by a distance of $k\zeta/r$. Simultaneously, the diffusive spread grows proportional to $\sqrt{D/r}$. In the stationary state, the drift and diffusion compensate each other, resulting in the balance equation $k\langle \zeta \rangle_s/r \sim \sqrt{D/r}$, leading to $\langle \zeta \rangle_s \propto \sqrt{Dr}/k$.

In contrast to the behavior of r , we find that $\langle \zeta \rangle_s$ decreases with increasing potential strength k . This is because the force pulling all particles toward the origin becomes stronger, thereby preventing the particles from escaping far from the origin. The decreasing behavior of $\langle \zeta \rangle_s$ with k is also consistent with the scaling behavior predicted by Eqs. (9) and (10). If $k \gg r$, $\langle \zeta \rangle_s$ decreases with exponent $-3/2$, i.e. $\langle \zeta \rangle_s \propto k^{-3/2}$, as shown in Eq. (9). In the opposite limit ($k \ll r$), $\langle \zeta \rangle_s$ decreases with exponent -1 , as seen in Eq. (10). These scaling behaviors are evident in Fig. 3(c).

Finally, we investigate the effect of diffusion coefficient D . A larger diffusion constant D allows particles to diffuse further, leading to growing $\langle \zeta \rangle_s$. As shown in

Fig. 3(d), we find that $\langle \zeta \rangle_s \propto \sqrt{D}$ (dotted line), which agrees with Eq. (8). This observation aligns with the intuitive understanding that the typical diffusion distance in the OUP is proportional to \sqrt{D} , thus increasing the resetting point similarly.

In summary, we have developed a general theoretical framework for group resetting, combining renewal theory and extreme value statistics. Unlike traditional resetting problems, our theory extends the resetting to collective behavior. This extension is achieved by deriving the renewal equation for P_r and incorporating it into the Fokker-Planck equation, leading to a master equation that describes the group CM dynamics. Analytical results for the stationary mean position reveal the impact of key parameters in group resetting on avoiding undesirable positions (e.g., $\zeta = 0$).

Our framework is broadly applicable to various group resetting problems. By appropriately defining P_r , it connects studies on fixed resetting distribution [2, 25–27], position-dependent resetting [1, 28, 29], simultaneous group resetting to origin [30] and time-dependent resetting based on particle trajectory history [31, 32]. Beyond existing research, our framework could be extended to artificial selection to identify key parameters such as bottleneck size, fitness, and selection intervals. By providing semi-analytical approximations, our theory reduces computational costs, enables efficient predictions, and helps design optimal selection protocols. Resetting tied to group thresholds may also offer new insights into allele frequencies and mechanisms that help populations avoid extinction.

Another potential application lies in control theory. Here, group resetting strategies can help mitigate undesirable outcomes in, for example, inventory fluctuations in warehouses with varying capacities or fluctuating cash levels across an ensemble of portfolios. These group-level resetting strategies have the potential to enhance resource utilization and improve the management

of shared constraints effectively.

As a final remark, our theory could be extended to a mixed strategy, where a fraction of particles reset to the currently best particle position while the remainder scatter across space. This approach reduces the risk of particles becoming trapped in local optima.

Acknowledgments—J.L., S.-G.Y., and L.L. acknowledge financial support from the Swedish Research Council (Grant No. 2017-03848 and 2021-04080). J.L and S.-G.Y are supported by postdoctoral fellowships from the Kempestiftelsen (Grant No. JCK22-0026.3) and the Carl Tryggers Stiftelse för Vetenskaplig Forskning (Grant No. CTS 22:2243), respectively. H.J.P is supported by the National Research Foundation of Korea grant funded by the Korea government (MSIT), Grant No. RS-2023-00214071, RS-2023-NR075951, and RS-2024-00460958.

* Corresponding author:hyejin.park@inha.ac.kr

† Corresponding author:ludvig.lizana@umu.se

- [1] M. Dahlenburg, A. V. Chechkin, R. Schumer, and R. Metzler, Stochastic resetting by a random amplitude, *Physical Review E* **103**, 052123 (2021).
- [2] M. R. Evans and S. N. Majumdar, Diffusion with optimal resetting, *Journal of Physics A: Mathematical and Theoretical* **44**, 435001 (2011).
- [3] A. Chechkin and I. M. Sokolov, Random search with resetting: a unified renewal approach, *Physical Review Letters* **121**, 050601 (2018).
- [4] X. Durang, S. Lee, L. Lizana, and J.-H. Jeon, First-passage statistics under stochastic resetting in bounded domains, *Journal of Physics A: Mathematical and Theoretical* **52**, 224001 (2019).
- [5] A. Pal and S. Reuveni, First passage under restart, *Physical Review Letters* **118**, 030603 (2017).
- [6] B. De Bruyne, J. Randon-Furling, and S. Redner, Optimization in First-Passage Resetting, *Physical Review Letters* **125**, 050602 (2020).
- [7] B. De Bruyne, J. Randon-Furling, and S. Redner, Optimization and growth in first-passage resetting, *Journal of Statistical Mechanics: Theory and Experiment* **2021**, 013203 (2021).
- [8] J. Davies and D. Davies, Origins and evolution of antibiotic resistance, *Microbiology and Molecular Biology Reviews* **74**, 417 (2010).
- [9] H. C. Neu, The crisis in antibiotic resistance, *Science* **257**, 1064 (1992).
- [10] J. M. Munita and C. A. Arias, Mechanisms of antibiotic resistance, *Virulence Mechanisms of Bacterial Pathogens*, 481 (2016).
- [11] J. M. Blair, M. A. Webber, A. J. Baylay, D. O. Ogbolu, and L. J. Piddock, Molecular mechanisms of antibiotic resistance, *Nature Reviews Microbiology* **13**, 42 (2015).
- [12] F. I. Arias-Sánchez, B. Vessman, and S. Mitri, Artificially selecting microbial communities: If we can breed dogs, why not microbiomes?, *PLoS Biology* **17**, e3000356 (2019).
- [13] Á. Sánchez, J. C. Vila, C.-Y. Chang, J. Diaz-Colunga, S. Estrela, and M. Rebolleda-Gomez, Directed evolution of microbial communities, *Annual Review of Biophysics* **50**, 323 (2021).
- [14] J. L. Thomas, J. Rowland-Chandler, and W. Shou, Artificial selection of microbial communities: what have we learnt and how can we improve?, *Current Opinion in Microbiology* **77**, 102400 (2024).
- [15] A. R. Mesquita, J. P. Hespanha, and K. Åström, Optimotaxis: A stochastic multi-agent optimization procedure with point measurements, in *International workshop on hybrid systems: Computation and control* (Springer, 2008) pp. 358–371.
- [16] J. Kennedy and R. Eberhart, Particle swarm optimization, in *Proceedings of ICNN'95-international conference on neural networks*, Vol. 4 (IEEE, 1995) pp. 1942–1948.
- [17] D. Wang, D. Tan, and L. Liu, Particle swarm optimization algorithm: an overview, *Soft Computing* **22**, 387 (2018).
- [18] G. E. Uhlenbeck and L. S. Ornstein, On the theory of the brownian motion, *Physical Review* **36**, 823 (1930).
- [19] C. Gardiner, *Stochastic methods*, Vol. 4 (Springer Berlin Heidelberg, 2009).
- [20] R. A. Fisher and L. H. C. Tippett, Limiting forms of the frequency distribution of the largest or smallest member of a sample, in *Mathematical proceedings of the Cambridge philosophical society*, Vol. 24 (Cambridge University Press, 1928) pp. 180–190.
- [21] A. Hansen, The three extreme value distributions: An introductory review, *Frontiers in Physics* **8**, 604053 (2020).
- [22] D. E. Cartwright and M. S. Longuet-Higgins, The statistical distribution of the maxima of a random function, *Proceedings of the Royal Society of London. Series A. Mathematical and Physical Sciences* **237**, 212 (1956).
- [23] M. R. Evans, S. N. Majumdar, and G. Schehr, Stochastic resetting and applications, *Journal of Physics A: Mathematical and Theoretical* **53**, 193001 (2020).
- [24] P. E. Kloeden, E. Platen, P. E. Kloeden, and E. Platen, *Stochastic differential equations* (Springer, 1992).
- [25] K. S. Olsen, Steady-state moments under resetting to a distribution, *Physical Review E* **108**, 044120 (2023).
- [26] F. Mori, K. S. Olsen, and S. Krishnamurthy, Entropy production of resetting processes, *Physical Review Research* **5**, 023103 (2023).
- [27] V. Mendez, R. Flaquer-Galmés, and D. Campos, First-passage time of a Brownian searcher with stochastic resetting to random positions, *Physical Review E* **109**, 044134 (2024).
- [28] O. Tal-Friedman, Y. Roichman, and S. Reuveni, Diffusion with partial resetting, *Physical Review E* **106**, 054116 (2022).
- [29] C. Di Bello, A. V. Chechkin, A. K. Hartmann, Z. Palmowski, and R. Metzler, Time-dependent probability density function for partial resetting dynamics, *New Journal of Physics* **25**, 082002 (2023).
- [30] M. Biroli, H. Larralde, S. N. Majumdar, and G. Schehr, Extreme Statistics and Spacing Distribution in a Brownian Gas Correlated by Resetting, *Physical Review Letters* **130**, 207101 (2023).
- [31] D. Boyer, M. R. Evans, and S. N. Majumdar, Long time scaling behaviour for diffusion with resetting and memory, *Journal of Statistical Mechanics: Theory and Experiment* **2017**, 023208 (2017).
- [32] S. N. Majumdar, S. Sabhapandit, and G. Schehr, Random walk with random resetting to the maximum position, *Physical Review E* **92**, 052126 (2015).